

UC Davis

UC Davis Previously Published Works

Title

Indole-3-lactic acid associated with Bifidobacterium-dominated microbiota significantly decreases inflammation in intestinal epithelial cells

Permalink

<https://escholarship.org/uc/item/5rz4g192>

Journal

BMC Microbiology, 20(1)

ISSN

1471-2180

Authors

Ehrlich, Amy M

Pacheco, Alline R

Henrick, Bethany M

et al.

Publication Date

2020-12-01

DOI

10.1186/s12866-020-02023-y

Copyright Information

This work is made available under the terms of a Creative Commons Attribution License, available at <https://creativecommons.org/licenses/by/4.0/>


Peer reviewed

RESEARCH ARTICLE

Open Access



Indole-3-lactic acid associated with *Bifidobacterium*-dominated microbiota significantly decreases inflammation in intestinal epithelial cells

Amy M. Ehrlich¹, Alline R. Pacheco^{2,3}, Bethany M. Henrick^{1,2,3}, Diana Taft^{2,3}, Gege Xu⁴, M. Nazmul Huda^{5,6}, Darya Mishchuk³, Michael L. Goodson¹, Carolyn Slupsky^{3,7}, Daniela Barile^{2,3}, Carlito B. Lebrilla⁴, Charles B. Stephensen^{6,7}, David A. Mills^{2,3} and Helen E. Raybould^{1*} 

Abstract

Background: *Bifidobacterium longum* subsp. *infantis* (*B. infantis*) is a commensal bacterium that colonizes the gastrointestinal tract of breast-fed infants. *B. infantis* can efficiently utilize the abundant supply of oligosaccharides found in human milk (HMO) to help establish residence. We hypothesized that metabolites from *B. infantis* grown on HMO produce a beneficial effect on the host.

Results: In a previous study, we demonstrated that *B. infantis* routinely dominated the fecal microbiota of a breast fed Bangladeshi infant cohort (1). Characterization of the fecal metabolome of binned samples representing high and low *B. infantis* populations from this cohort revealed higher amounts of the tryptophan metabolite indole-3-lactic acid (ILA) in feces with high levels of *B. infantis*. Further in vitro analysis confirmed that *B. infantis* produced significantly greater quantities of the ILA when grown on HMO versus lactose, suggesting a growth substrate relationship to ILA production. The direct effects of ILA were assessed in a macrophage cell line and intestinal epithelial cell lines. ILA (1-10 mM) significantly attenuated lipopolysaccharide (LPS)-induced activation of NF- κ B in macrophages. ILA significantly attenuated TNF- α - and LPS-induced increase in the pro-inflammatory cytokine IL-8 in intestinal epithelial cells. ILA increased mRNA expression of the aryl hydrogen receptor (AhR)-target gene CYP1A1 and nuclear factor erythroid 2-related factor 2 (Nrf2)-targeted genes glutathione reductase 2 (GPX2), superoxide dismutase 2 (SOD2), and NAD(P) H dehydrogenase (NQO1). Pretreatment with either the AhR antagonist or Nrf-2 antagonist inhibited the response of ILA on downstream effectors.

Conclusions: These findings suggest that ILA, a predominant metabolite from *B. infantis* grown on HMO and elevated in infant stool high in *B. infantis*, and protects gut epithelial cells in culture via activation of the AhR and Nrf2 pathway.

Keywords: Milk oligosaccharides, Aryl-hydrocarbon receptor, Nuclear factor erythroid 2-related factor 2, Indole-3-lactic acid

* Correspondence: heraybould@ucdavis.edu

¹Department of Anatomy, Physiology and Cell Biology, School of Veterinary Medicine, University of California, Davis, CA 95616, USA

Full list of author information is available at the end of the article



© The Author(s). 2020 **Open Access** This article is licensed under a Creative Commons Attribution 4.0 International License, which permits use, sharing, adaptation, distribution and reproduction in any medium or format, as long as you give appropriate credit to the original author(s) and the source, provide a link to the Creative Commons licence, and indicate if changes were made. The images or other third party material in this article are included in the article's Creative Commons licence, unless indicated otherwise in a credit line to the material. If material is not included in the article's Creative Commons licence and your intended use is not permitted by statutory regulation or exceeds the permitted use, you will need to obtain permission directly from the copyright holder. To view a copy of this licence, visit <http://creativecommons.org/licenses/by/4.0/>. The Creative Commons Public Domain Dedication waiver (<http://creativecommons.org/publicdomain/zero/1.0/>) applies to the data made available in this article, unless otherwise stated in a credit line to the data.

Background

Numerous studies have correlated breastfeeding with significant decreases in infant morbidity and mortality. Breast milk provides high levels of innate and adaptive immune factors that have direct antibacterial and antiviral activity [1], however, it also provides high levels of free sugars known as human milk oligosaccharides (HMOs) [2]. HMOs make up the third largest component of breast milk yet are indigestible by enzymes present in the infant gut. HMOs likely have many functions; they can mimic receptor sites for pathogenic microbes in the gut [3, 4] and have direct effects on intestinal epithelial cells [4, 5]. However, HMOs also provide the growth substrate for beneficial commensal bacteria, such as *Bifidobacterium* species that are equipped with the cellular machinery to breakdown and utilize these complex substrates as an energy source [2, 6–8].

Bifidobacterium longum subsp. *infantis* (*B. infantis*) is an important early colonizer and one of the predominant species in the intestinal microbiome of breastfed infants [9, 10]. *B. infantis* expresses an impressive repertoire of oligosaccharide transporters and glycosyl hydrolases required to consume complex sugars internally [11, 12] which provides a growth advantage [13]. A recent study demonstrated how supplemented *B. infantis* can dominate the gut of breastfed infants, consume HMOs and dramatically modulate the colonic pH via production of acetic and lactic acids [14]. Other studies have suggested *B. infantis* to be beneficial to the infant in numerous ways, including providing antimicrobial properties, improving intestinal permeability and reducing inflammation in the gut [15–20].

In addition to any direct effects that *B. infantis* or HMOs have on the host, there is good evidence to suggest that bacterial metabolites can also have beneficial effects on host physiology. Various metabolites, including short chain fatty acids (SCFA), phenylalanine metabolites and tryptophan metabolites have been shown to have broadly beneficial effects on host health [21, 22]. We have previously shown that direct interaction of *B. infantis* grown on HMOs with intestinal epithelial cells significantly reduced markers of inflammation by comparison to *B. infantis* grown on either glucose or lactose [17]. This suggests that the carbon source changes the composition of bioactive metabolites secreted from *B. infantis*. However, the precise identity of the metabolites mediating these effects and the mechanism of their action on the intestinal mucosa remains largely unknown. We hypothesized that growth of *B. infantis* on HMOs compared to simple carbohydrates such as lactose, results in secretion of bioactive metabolites that influence the gastrointestinal tract of the host. Therefore, to identify the effect of carbon source on metabolite composition, *B. infantis* was grown either on HMOs or lactose as the sole carbon source and NMR was used to identify metabolites. We sought to identify the mechanism by which a particular metabolite, indole-3-

lactic acid (ILA), that was enriched when *B. infantis* was grown on HMOs, inhibits release of inflammatory cytokines in intestinal epithelial cells in vitro. Further, we determined the pathway by which ILA acts, showing activation of the aryl hydrocarbon receptor (AhR) and nuclear factor erythroid 2-related factor 2 (Nrf2)-targeted genes. Finally, the concentration of ILA and short chain fatty acids (SCFAs) was measured in fecal samples from breastfed infants that had a predominantly *Bifidobacterium*-dominated intestinal microbiome. The data show that ILA is in high concentration in the feces of infants with a *Bifidobacterium*-dominated intestinal microbiome, is an enriched metabolite of *B. infantis* when grown of HMOs and produces marked anti-inflammatory effects via activation of the AhR pathway.

Results

Indole-3-lactic acid is elevated in infant fecal samples with a high compared to low abundance of *B. infantis*

Previously, we characterized a cohort of Bangladeshi breast fed infants revealing a high (dominating) level of *B. infantis* occurring frequently among this cohort (1, 23). To examine if this high bifidobacterial content was associated with specific metabolic products, we binned fecal samples for high and low bifidobacterial content and performed mass spectrometry-based metabolomics. Fecal samples were selected based on total *Bifidobacterium* and *B. infantis* relative abundance with 9 samples containing the highest abundance and 9 with the lowest abundance [23]. The low *Bifidobacterium* samples contained an average of 0.96% *Bifidobacterium* (median 1%; standard deviation of 0.7%), and will be referred to as 'low *Bifidobacterium*' group. The high *Bifidobacterium* samples had an average of 93.56% (median 92%; standard deviation 2.55%) *Bifidobacterium* and will be referred to as 'high *Bifidobacterium*' group. In this high *Bifidobacterium* group, the next most abundant genera were represented by *Streptococcus*, *Lactobacillus* and *Enterococcus*. Conversely, the 'low *Bifidobacterium*' fecal samples were populated with various genera, including predominantly *Streptococcus* and *Enterococcus* genera (Fig. 1a). In the samples with high *Bifidobacterium* abundance, the mean relative abundance of *B. infantis* represented 97.22% (median 1.0; standard deviation 6.53%) from the total *Bifidobacterium* population. The gut microbial weighted (betadisper: F.model = 4.96, $P = 0.048$; ADONIS: F.model = 34.0, $R^2 = 0.680$, $P < 0.01$) and unweighted (betadisper: F.model = 0.446, $P = 0.50$; ADONIS: F.model = 2.87, $R^2 = 0.152$, $P < 0.01$) β diversity was significantly different between high and low *Bifidobacterium* groups (Fig. 1b and c).

Short chain fatty acids and the indole derivative ILA were measured in the 18 infant fecal samples using mass spectrometry. The concentration of ILA was significantly elevated in fecal samples from infants with a high versus low *Bifidobacterium*-dominated microbiome (Fig. 1d, e;

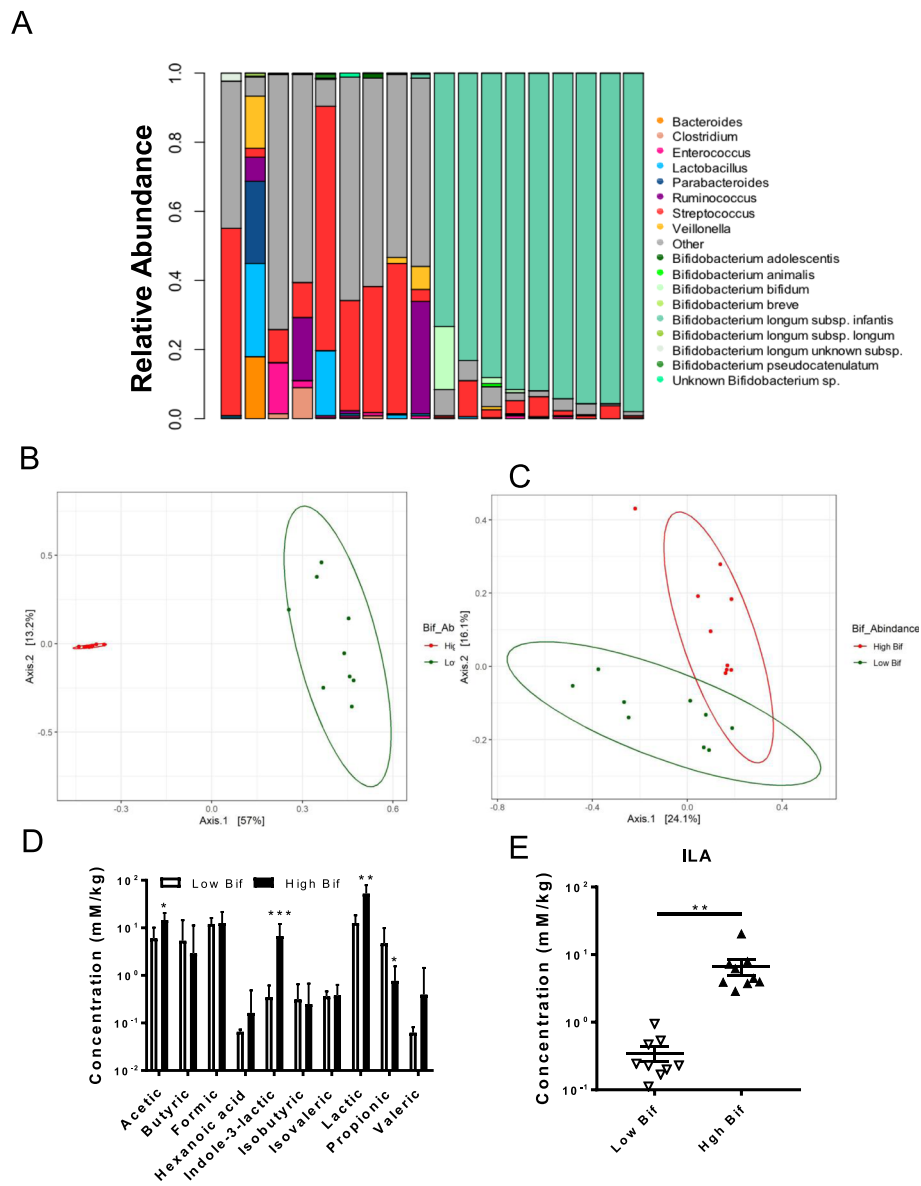


Fig. 1 Increased ILA production in fecal samples from infants with high levels of bifidobacteria. Determination of microbiota in infant fecal samples using 16S, Bif-TRFLP, and BLIR assays. **a** Fecal samples showed low and high distributions of *Bifidobacterium* among breast fed infants ($n = 18$) previously characterized (1). In fecal samples with a high level of *Bifidobacterium*, the distribution of species and subspecies is shown in different shades of green (note *B. longum* subsp. *infantis* dominating all of the high *Bifidobacterium* feces). **b** PCoA plots of weighted and **c** unweighted β diversity was significantly different between high and low *Bifidobacterium* groups. **d** Metabolite analyses of infant fecal samples by LC-MS/MS (72). **e** High *Bifidobacterium* samples showed highly significant differences in ILA production ($p < 0.0001$) compared to low *Bifidobacterium* samples. Student t-test was used to determine significance with corresponding P values considered statistically significant in $*p < 0.05$, $**p < 0.01$, $***p = 0.0001$

$P < 0.0001$). The *B. infantis*-dominated microbiome population produced a greater than 19-fold increase in ILA concentration compared to the low-*Bifidobacterium* dominated infant microbiome (Fig. 1d, e);). The concentration of acetic and lactic acid was significantly increased in the fecal samples from the high versus low *Bifidobacterium* groups (Fig. 1d; $P = 0.0353$, $P = 0.0095$, respectively). There was also a significant decrease in the concentration of propionic acid in the high versus low

Bifidobacterium groups ($P = 0.049$). There was no significant difference in the concentrations of the other detectable SCFA (butyric, formic, isobutyric, and valeric) between the high versus low bifidobacterial groups.

Growth on HMOs versus lactose determines *B. infantis* metabolite profile in vitro

The observation of increased ILA from *B. infantis*-dominated feces suggested this metabolite emanated from *B.*

infantis. One mechanism by which *B. infantis* dominates the infant gut is through the consumption of complex human milk oligosaccharides (HMOs) in milk (15). Production of acetate, lactate and formate by *Bifidobacterium* species has previously been shown to be dependent on the carbon source in the growth medium [24] but how growth on HMOs influences production of metabolites from *B. infantis* has not been described. In order to determine the differences in the metabolites produced by *B. infantis* grown on two different carbon sources, we performed untargeted metabolomic analysis of the supernatant from *B. infantis* grown in chemically defined RPMI 1640 medium supplemented with either lactose or HMO. *B. infantis* grown on HMO or lactose produced a large number of metabolites, including amino acids, organic acids and carbohydrates (Supplemental Fig. 1). The data show significantly increased production of acetate, glutamate, glycerol, glycine, indole-3-lactate, leucine, pyruvate, and valine in HMO-supplemented compared to lactose-supplemented medium (Supplemental Fig. 1; all $P < 0.0001$). HMO-supplemented growth of *B. infantis* produced greater than 4-fold more ILA compared to bacteria grown in lactose-supplemented media (Supplemental Fig. 1, insert; $P < 0.0001$), suggesting that production of ILA is increased when *B. infantis* is consuming milk glycans.

Recently, it was shown that supplementing the diet of weanling piglets with tryptophan decreased expression of inflammatory markers in the large intestine [25] which may be due to the increased production of tryptophan metabolites. ILA is a known catabolite of tryptophan [26] and ILA was significantly elevated when *B. infantis* was grown on HMOs and in the feces containing high levels of *B. infantis*. Therefore, we investigated whether addition of tryptophan would alter metabolite composition when *B. infantis* was grown in RPMI 1640

supplemented with either HMO or lactose in the presence of increasing concentrations of tryptophan. Metabolomics analysis revealed that tryptophan produced an increase in the production of glutamate, glycerol, ILA, leucine, and valine in HMO-supplemented compared to lactose-supplemented medium (Supplemental Fig. 1; $P = 0.0001$, $P = 0.0077$, $P = 0.0009$, $P = 0.0001$, $P = 0.0040$, respectively). Increasing the tryptophan also significantly increased the catabolism of 3'FL, 6'SL, cysteine, glucose and LNnT in HMO (Fig. 2: $P = 0.0037$; $P < 0.0001$; $P = 0.0003$; $P < 0.0001$; $P < 0.0001$, respectively).

Given the differential amounts of ILA between feces containing high versus low abundance of *B. infantis*, combined with the increase in ILA production from *B. infantis* grown on HMO, and its increase concentration in the presence of tryptophan in the growth medium, ILA appeared to be an appropriate target for further study. ILA production differs from the other significant metabolites that were also increased by growth on HMOs compared to lactose as it is not directly involved in energy metabolism. ILA and other tryptophan metabolites are known to produce beneficial effects in the host [27–29]. We hypothesized that ILA may be responsible, at least in part, for the anti-inflammatory effects associated with *B. infantis*.

Indole-3-lactic acid decreases endotoxin-induced activation of macrophages, and release and expression of IL-8 in intestinal epithelial cells

To test for a potential anti-inflammatory role of ILA in the intestinal mucosa, studies were performed in a macrophage cell line and intestinal epithelial cell lines in vitro. Initial experiments to show a potential anti-inflammatory action was performed in the mouse macrophage reporter cell line RAW blue cells. Subsequent experiments were performed in the intestinal epithelial cell lines Caco2 and

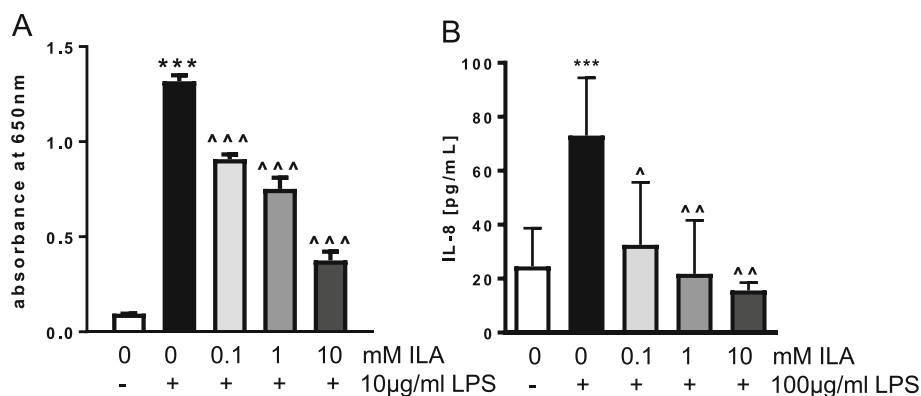


Fig. 2 ILA inhibits LPS-induced inflammation in macrophage and intestinal epithelial cells. **a** SEAP activity in RAW blue macrophage cells exposed to media alone, LPS alone, or with different concentrations of ILA for 1 h prior to addition of LPS. **b** IL-8 from IECs exposed to media alone, LPS alone for 18 h or with different concentrations of ILA for 1 h prior to LP. Data is expressed as mean \pm SEM, $n = 3-7$ and Student t-test was used to determine significance with corresponding P values considered statistically significant; *** $p < 0.0001$ compared to no treatment control or \wedge $p < 0.05$, $\wedge\wedge$ $p < 0.01$, $\wedge\wedge\wedge$ $p < 0.0001$ compared to LPS alone

HT-29. Two different cell lines were used to ensure that the anti-inflammatory response to ILA could be reproduced in both cell lines. Experiments on dissecting the AhR and Nrf2 pathway were performed in HT-29 cells.

Given the central role NF κ B plays in the activation of innate immune responses [30], we first evaluated the ability of ILA to modulate LPS-induced immune activation using the mouse macrophage reporter cell line RAW blue cells. Overnight treatment of the mouse RAW blue cells with LPS (10 μ g/ml) significantly increased activation of NF κ B (Fig. 2a, $P < 0.0001$); pretreatment with ILA (0.1 mM–10 mM) significantly inhibited LPS-induced NF κ B activation in a dose-dependent manner (Fig. 2a; $P < 0.0001$). Similar anti-inflammatory effects were seen in Caco-2 cells; pretreatment with ILA significantly decreased LPS-induced production of IL-8 (Fig. 2b; $P = 0.0006$; $P = 0.0021$).

Similar anti-inflammatory actions were seen in HT-29 cells. LPS is a potent stimulus for release of the pro-inflammatory cytokine tumor necrosis factor-alpha (TNF- α) [31], therefore, we determined the ability of ILA to decrease inflammatory responses to TNF- α . HT-29 cells were incubated with TNF- α (20 ng/ml) for 1 h in

the absence (control) or presence of ILA (0.1–10 mM). Cellular responses were analyzed using qPCR for IL-8 (immune activation), serotonin transporter (SERT) and tryptophan hydroxylase 1 (TPH1) (ILA is an indole derivative which have previously been shown to interact with serotonin receptors), and β -defensin 2 (hBD2; antimicrobial defense protein previously shown to be activated by bifidobacteria). TNF- α induced a robust increase in IL-8 mRNA expression ($P < 0.0001$) but there was no change in expression of SERT, hBD2, or TPH1 (Fig. 3). The increase in expression of IL-8 induced by TNF- α was significantly decreased by treatment with ILA (Fig. 3a; $P < 0.0001$ for 0.1, 1, and 10 mM ILA); there was no significant difference in expression of IL-8 between cells treated with TNF- α in the presence of ILA and those treated with vehicle alone (Fig. 3a, $P = 0.061$, $P = 0.90$ $P = 0.59$ for 0.1, 1, and 10 mM ILA, respectively). Further, expression of SERT and hBD2 were significantly increased in cells treated with ILA (10 mM) (Fig. 4b, c, $P = 0.016$ and $P = 0.042$). Expression of TPH1 was not affected by treatment with TNF- α in the presence or absence of ILA (Fig. 3d).

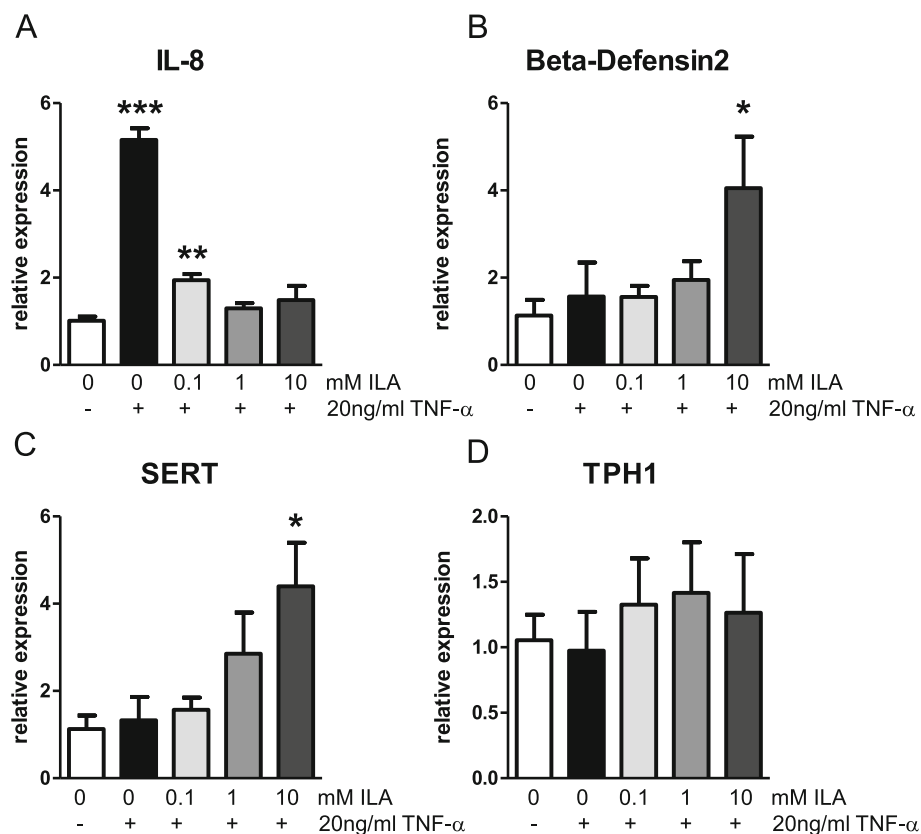


Fig. 3 ILA inhibits TNF- α induced inflammation in intestinal epithelial cells. mRNA expression in IEC exposed to media alone, TNF- α or TNF- α in the presence of different concentrations of ILA for 1 h. **a** IL-8, **b** beta-defensin2, **c** SERT and **d** TPH1 mRNA expression. Data is expressed as mean \pm SEM, $n = 6$ for each condition and Student t-test was used to determine significance with corresponding P values considered statistically significant (* $p < 0.05$, ** $p < 0.01$, *** $p < 0.0001$)

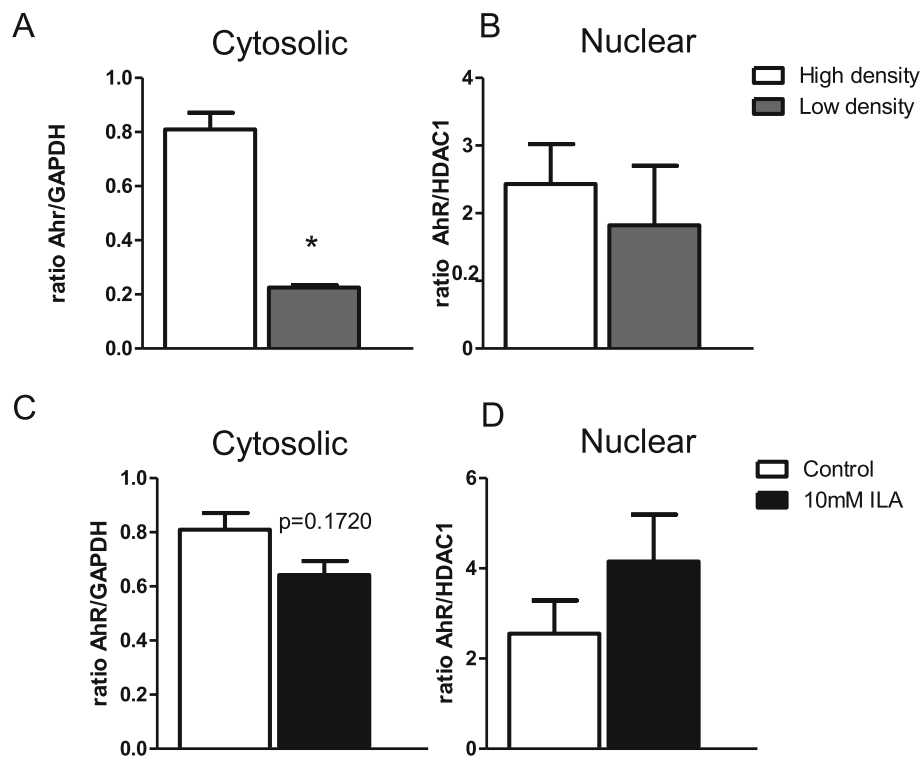


Fig. 4 Cell density or presence of ILA affects AhR localization. **a** AhR cytosolic protein expression in IEC plated at high density (100% confluency) versus low confluency (50% confluency). **b** AhR nuclear protein expression in high and low density IECs ($p = ns$). **c** AhR cytosolic protein expression in high density IEC treated with ILA. **d** AhR nuclear protein expression in high density IEC treated with ILA. Protein was pooled from 6 individual plates of cells. Data is expressed as mean \pm SEM; $n = 2$ and student t-test was used to determine significance with corresponding P values considered statistically significant in * $p < 0.05$, ** $p < 0.01$, *** $p < 0.0001$

ILA activates the aryl hydrocarbon receptor (AhR) and downstream nuclear factor erythroid-derived 2-like 2 (Nrf2) pathway in intestinal epithelial cells

There is evidence that tryptophan catabolites contribute to gut homeostasis via modulating mucosal immune responses through an AhR signaling pathway [26, 32]. AhR is a nuclear receptor that when activated translocates to the nucleus to increase transcription of AhR-regulated genes. Previous work has indicated that AhR changes its cellular location based on cell density [33]. To confirm this occurs in intestinal cells, we measured protein expression of AhR by western blot in cytosolic and nuclear extracts from Caco-2 cell cultured at either low (50% confluency) or high (100% confluency). Consistent with published data from other cell types [28], intestinal epithelial cells grown at high density have increased cytosolic AhR compared to cells plated at low density (Fig. 4a, $P = 0.01$). For a preliminary test that ILA can activate AhR, AhR expression was measured in the nuclear and cytosolic fractions in Caco-2 cells grown at high density in response to ILA. There was a trend for increased AhR expression in the nucleus and decreased AhR expression in the cytosol, indicating that ILA may activate AhR (Fig. 4c, d).

In order to further understand the potential role of AhR in the anti-inflammatory response to AhR, we used HT-29 cells. Treatment of HT-29 cells with ILA (0.1–10 mM) induced a robust increase of mRNA transcript of AhR regulated gene cytochrome p450 1A1 (CYP1A1), which was significantly decreased by pretreatment with the AhR antagonist (CH-223191; 10 μ M) (Fig. 5a, $P = 0.0000003$) or Nrf2 antagonist (SML1833; 4 μ M) (Fig. 5a, $P = 0.0001066$). There is considerable evidence for cross talk between the AhR and Nrf2 pathways, which led us to test activation of the Nrf2 pathway [34]. Upon exposure to ILA, there were dose-dependent increases in Nrf2 activated genes glutathione peroxidase 2 (GPX2) and super oxide dismutase 2 (SOD2) and an increase in NAD(P) H dehydrogenase (NQO1) was observed. Inhibition of either AhR or Nrf2 completely suppresses ILA activation of GPX2, SOD2, and NQO1 genes (Fig. 5a-d, all $P < 0.001$).

To test if the AhR or Nrf2 pathway is involved in the ILA-induced suppression of pro-inflammatory IL-8 production, HT-29 cells were treated with TNF- α (20 ng/ml) and ILA (0.1–10 mM) in the presence of either an AhR antagonist or a Nrf2 inhibitor. ILA treatment produces a dose-dependent decrease in TNF- α -induced IL-

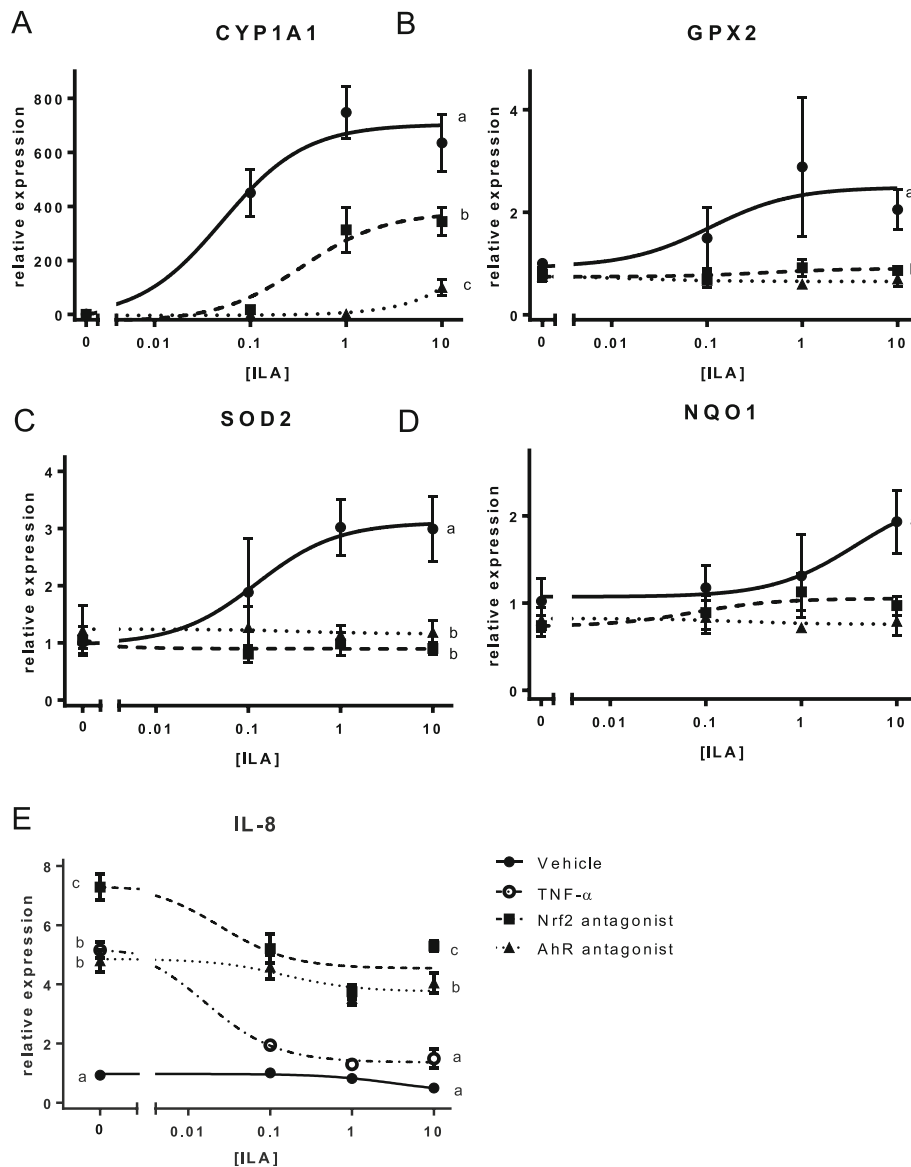


Fig. 5 AhR or Nrf2 inhibition prevents ILA-induced response in intestinal epithelial cells. mRNA expression in IEC treated with ILA alone or with AhR or Nrf2 antagonist. **a** CYP1A1 **b** GPX2 **c** NQO1 **d** SOD2 **e** IL-8 mRNA. Data is expressed as mean ± SEM with $n = 6-8$ of relative expression values fitted with a 3-parameter dose response curve vs the log-transformed ILA concentration (Prism, v. 8.0, GraphPad Software, San Diego, CA). Statistical significance of the effect of each treatment on the means of relative expression of each target gene at the highest ILA concentration (10 mM) was determined using a one-way ANOVA analysis with a TukeyHSD posthoc comparison (R, version 3.5.2 (1)). For IL-8, the statistical differences between the means in the absence of ILA was also determined by this method. Different letters represent significantly different means. A summary of statistics can be found in Supplemental Table 3

8 expression which is inhibited by pretreatment with either an AhR antagonist or a Nrf2 inhibitor (Fig. 5e, all $P < 0.0001$).

Discussion

Development of the microbiome starts at birth and there is evidence for the importance of a *Bifidobacterium*-dominated microbiome in breastfeeding infants to provide protection from inflammatory diseases [35, 36]. The

enrichment of *B. infantis* in breastfed infants is believed to be driven by its ability to completely digest complex milk sugars (HMOs) leading to the conclusion that this subspecies is a keystone bacterium of the infant intestine [11, 12, 37]. Previous studies have reported on the anti-inflammatory effects of *B. infantis* both in vivo and in vitro [38, 39]. How *Bifidobacterium* are mediating their effects is not well understood but previous studies point to bioactive HMO metabolites produced by *Bifidobacterium*. Therefore,

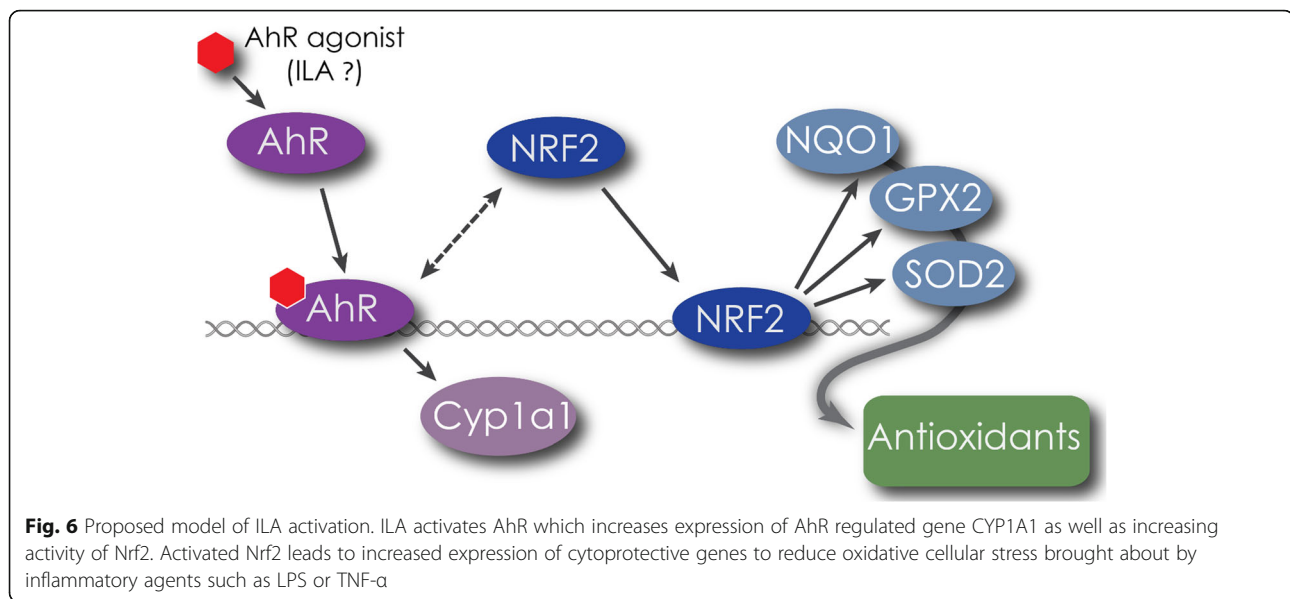
the purpose of the present study was to identify the metabolites produced by *B. infantis* that have anti-inflammatory effects and determine the pathways by which they act. Here we show, by comparing metabolites generated from *B. infantis* grown on HMO with specific metabolites found in the fecal samples from breast fed babies with a *B. infantis*-dominated microbiome, that ILA was significantly enriched in both sample sets. Further, our data shows that ILA significantly decreased production of the pro-inflammatory cytokine IL-8 in intestinal epithelial cell lines and decreased activation of macrophage cell line. In intestinal epithelial cells, the ability of ILA to decrease TNF- α -induced IL-8 expression was significantly reduced by pretreatment with either an AhR or Nrf2 antagonist and ILA treatment was associated with an increased expression of AhR and Nrf2 related genes. Taken together, these data show that a metabolite from *B. infantis*, which is both enriched during growth on HMOs as well as found in fecal samples from high-*Bifidobacterium* dominated infant fecal samples, can produce anti-inflammatory action via the AhR and Nrf2 pathway.

Initial work on AhR focused on its role in mediating the effects of toxic chlorinated dioxins and similar halogenated aromatic hydrocarbon compounds on many cell types and tissues [40], but it is evident that this receptor also plays a crucial role in regulating intestinal homeostasis. For example, AhR deficiency impairs intestinal stem cells from properly repairing after tissue damage [41]. Further, mice with dysregulated AhR regulated gene CYP1a1 mimicking an AhR-deficient state exhibited significantly decreased ability to clear infections from enteric pathogens [42]. Interestingly, when the AhR ligand indole-3-propionic acid (IPA) is administered to mice with DSS-induced colitis, there is reduction in pro-inflammatory cytokines and attenuation of disease severity. This is proposed to be the result of AhR mediated IL-10 induction [32]. There are a number of other downstream mediators that have been proposed, including production of anti-inflammatory cytokines such as IL-22 from intestinal immune cells, differentiation of CD4 + Foxp3 T cells, and more recently, increased expression of anti-inflammatory cytokine receptors [19, 32, 43, 44]. Numerous plant polyphenols such as polydatin, quercetin, reutin, and resveratrol [45], and an increasing list of metabolites produced from microbes such as IPA, indole-3-acetaldehyde, and indole-3-aldehyde [28], known to exert beneficial effects have been recently shown to act through AhR [29]. However, specific metabolites produced from *Bifidobacterium* are just recently beginning to be identified as anti-inflammatory mediators acting through AhR [46]. Blood samples from humans administered *B. infantis* have shown in increased secretion of IL-10 and expression of Foxp3 [47] suggesting that *B. infantis* leads to AhR activation though it is not clear whether it is a direct or indirect effect.

Our data suggests additional beneficial effects of activating AhR are mediated through its cross talk with Nrf2 pathway. The Nrf2 pathway is associated with cytoprotective, redox sensitive pathways conferring resistance to oxidative stress [34, 48]. One particular Nrf2 agonist, sulforaphane, has been shown to attenuate inflammation and disease in LPS-challenged mice [49] and in a chemically-induced model of diabetes [50] via similar mechanisms as we have observed in the current study, with ILA suppressing NF- κ B activation and decreasing production of pro-inflammatory cytokines. The anti-inflammatory effects observed in this study are in corroboration with recent findings demonstrating protection against necrotizing enterocolitis with ILA through AhR [46] but here we provide evidence to also suggest a role for Nrf2. The potential interaction of ILA with these pathways is depicted in Fig. 6.

It has been previously demonstrated that ILA is produced by 51 species of *Bifidobacterium* incubated with tryptophan so it was not surprising to find increased ILA production with increasing concentrations of tryptophan [19]. High concentrations of tryptophan have been shown in human milk during the neonatal period [51]. Recent reports highlight the significance of tryptophan by showing anti-inflammatory effects in the colon of piglets ingesting a diet supplemented with tryptophan [25]. Thus, in order to evaluate whether the presence of additional tryptophan influences metabolite production by *B. infantis* grown on HMO, the concentration of tryptophan in growth media was increased. With increased tryptophan, we found increased production of ILA. In light of the observation that TNBS-induced colitis is increased in severity in SERT-deficient mice, we looked at whether the potential beneficial effects of the *B. infantis* metabolite ILA might also have effects on the serotonergic system [52, 53]. ILA had no effect on TPH1 expression, the enzyme that catalyzes the production of 5-HT from tryptophan, in intestinal epithelial cells. However, there was a significant upregulation of SERT; increased SERT could decrease inflammation by increasing transport of 5-HT away from the mucosa.

Similarly, ILA increases expression of human beta-defensin2 (hBD2). Lower levels of hBD2 have been found in patients with Crohn's disease, perhaps due to a reduced ability to induce expression [54] or due to decreased number of copies of the hBD2 gene [55]. It does seem plausible that ILA could interact with the serotonergic system since particular residues in the 5-HT_{1B} binding pockets specifically bind the indole ring common to ILA and serotonin [56]. Additionally, it is possible ILA engages the vitamin D receptor to increase hBD2 expression. Previous reports have described cross-talk with NRF2 agonist sulforaphane and the vitamin D receptor leading to induced expression of hBD2 through this transcription factor in intestinal cells in culture [57].



Conclusion

In conclusion, these results identify significantly increased production of ILA by bifidobacterial-dominated breast fed infants. This is in line with previous publications that show ILA as a predominant tryptophan catabolite produced by many species in the *Bifidobacterium* genus in vitro [19]. Critically, we show the metabolite profile produced by *B. infantis* grown in vitro depends on growth on HMO compared to lactose, and production of the key metabolite ILA being significantly increased when HMO is available for *B. infantis*. The data shown here indicates that intestinal epithelial cells exposed to ILA produced significantly less pro-inflammatory cytokine in a dose-dependent manner providing a possible mechanism for the anti-inflammatory effects and improved intestinal health observed in *Bifidobacterium*-dominated breast fed babies. The observation that ILA activates AhR and Nrf2 and that this activation is required for ILA to regulate pro-inflammatory genes provides additional key mechanistic insight into how *Bifidobacterium* and HMO may be eliciting their anti-inflammatory effects to improve intestinal health. Together, these results have important implications for our fundamental understanding of metabolite production by specific bacterial species and support the notion that ILA might be considered an important regulator of intestinal inflammation in the breastfeeding infant. These, and other recent data may provide critical insight for generation of probiotics and dietary recommendations.

Methods

Infant fecal samples collection

We utilized 18 fecal samples (9 with highest and 9 with lowest *Bifidobacterium* abundance) originally collected

as part of a larger trial in Bangladesh (clinicaltrials.gov identifier: NCT01583972 and NCT02027610). Detailed study design, sample collection procedures, and initial results have been reported earlier [23, 58–60]. Briefly, parents of infants born at the Maternal and Child Health Training Institute in Dhaka, Bangladesh were approached during the third trimester of pregnancy and informed consent was obtained. Infants were supplemented with a high dose vitamin A within 48 h of birth and stool samples were collected at 6 weeks of age and stored at -70°C , as part of the original study. The study was approved by the Ethical Review Committee of the International Centre for Diarrheal Disease Research, Bangladesh (ICDDR,B) and by the Human Studies Committee of the World Health Organization.

Infant gut microbiota assay

Whole stool samples were collected and were frozen at -70°C until assay. Detailed of the 16S assay including randomization, V4 amplicon library preparation, and bioinformatics analysis have been reported previously [59]. In brief, stool DNA samples were randomized, total fecal DNA was extracted and mixed template 16S V4 amplicon library was prepared using the primer sets (515F and barcoded 806R) [61] and sequenced using the Illumina MiSEQ platform with 2x250bp paired-end sequencing. Raw paired-end sequences were analyzed using the open-source software Quantitative Insights Into Microbial Ecology (QIIME) version 1.8 [62]. Taxonomy was assigned using the Greengenes May 2013 reference database [63] at the threshold of 97% pairwise identity. To estimate *Bifidobacterium* species and subspecies, we used Bif-TRFLP (*Bifidobacterium*-specific terminal restriction fragment length polymorphism)

assay and BLIR (*Bifidobacterium longum* subsp. *longum-infantis* Ratio) assay, respectively, as has been reported earlier [23]. The relative abundance of the infant's gut microbiota presented as combined results from 16S QIIME, Bif-TRFLP, and BLIR assay. The 16S sequence data is available at NCBI Sequence Read Archive (SRA) database under the BioProject ID "PRJNA636907" and "PRJNA636905".

Fecal metabolite analysis by LC-MS/MS

Pre-weighed fecal samples are diluted, homogenized, and centrifuged before extraction of the fecal supernatants. 20 μ L of supernatant is reacted with 20 μ L of 200 mM N-(3-Dimethylaminopropyl)-N'-ethylcarbodiimide hydrochloride (1-EDC HCl) in 5% pyridine and 40 μ L of 100 mM 2-nitrophenylhydrazine (2-NPH) in 80% ACN/H₂O (v/v) with 50 mM HCl. The samples were reacted for 30 min at 40 °C before being diluted with 400 μ L of 10% ACN/H₂O. Samples were centrifuged for 20 min before transferring to a 96-well injection plate for QqQ LC-MS/MS analysis. Dynamic MRM method was used in positive mode for detection and quantitation of the compounds. The quantification is absolute concentration and are shown as mmol/kg of original fecal sample wet weight [64].

Bacterial growth and supernatant preparation

Single colony isolates of *B. infantis* ATCC 15697 were grown from frozen stocks on de Mann, Rogosa, and Sharpe medium (MRS) supplemented with 2% (wt/vol) carbon source and 0.25% (wt/vol) L-cysteine (Sigma-Aldrich) for 18 h, centrifuged for 10 min at 4000 rpm, re-suspended in glucose-free RPMI 1640 (Life Sciences) then inoculated in three biological replicates at 1:100 ratio in RPMI 1640 (chemically defined) containing 2% of human milk oligosaccharides (HMO) previously purified in the UCD Milk Processing Lab or lactose (control). To obtain lactose-free HMOs, a purification approach of pooled donor milk based on lactose hydrolysis, yeast consumption of the resulting monosaccharides and further clean-up and concentration by sequential membrane filtration was used [65]. The freeze-dried powder was characterized by mass spectrometry and analyzed by high-performance anion-exchange chromatography with pulsed amperometric detection using a previously published method tailored for oligosaccharide quantification in milk [66] (Supplemental Table 1). *B. infantis* was incubated at 37 °C until early stationary phase under anaerobic conditions (5% carbon dioxide, 5% hydrogen, and 90% nitrogen) in a vinyl anaerobic chamber (Coy Laboratory Products). Bacterial growth was monitored by optical density (OD₆₀₀) and an aliquot of the bacterial suspension was taken for determination of the bacterial counts by plating on MRS Agar. Sample preparation for

exometabolome analysis was performed as described by Smart et al [67]. Cell-free supernatants were obtained by centrifuging the bacterial cultures at 4000 rpm for 15 min, followed by filtration using 0.22 μ m filters (Millipore) to remove microbial cells and addition of 0.2 μ mol per sample of isobutyric acid as internal standard. Samples were distributed in 100 μ L aliquots and stored at -80 °C until processing. Uninoculated growth media was collected and used as controls for exometabolome analysis.

NMR spectroscopy

Frozen supernatant samples were thawed and filtered through 3000 MW cutoff filters to remove lipids and proteins. Samples were prepared by addition of 65 μ L of an internal standard containing 5 mM DSS-d6 (2,2,3,3,4,4-d6-3-(trimethylsilyl)-1-propane sulfonic acid), 0.2% NaN₃ in 99% D₂O to 585 μ L of supernatant. Sample pH was subsequently adjusted to 6.8 through the addition of small amounts of NaOH or HCl. 600 μ L aliquots were transferred to 5 mm Bruker NMR tubes, and stored at 4 °C until NMR acquisition which was within 24 h of sample preparation. NMR spectra were acquired as previously described by He et al. [68] using a Bruker Avance 600 MHz NMR equipped with a SampleJet autosampler using a NOESY-presaturation pulse sequence (noesypr) at 25 °C. Once acquired, all spectra were processed as described [68] using Chenomx NMR Suite v6.1 Processor (Chenomx Inc., Edmonton, Canada). Metabolite quantification was achieved using the 600-MHz library from Chenomx NMR Suite v6.1 Profiler, which uses the concentration of a known reference signal (in this case DSS) to determine the concentration of individual compounds. Metabolites were quantified in micro-molar (μ M) units and exported from Chenomx for statistical analysis. Metabolite concentrations were normalized to bacterial CFU and were calculated relative to the concentration found in the growth media whereby a positive number indicates microbial production and a negative indicates consumption.

Cell lines and reagents

RAW-Blue cells (InvioGen), a mouse macrophage cell line engineered with secreted embryonic alkaline phosphatase (SEAP) reporter system, was used to evaluate LPS-induced NF κ B activation in the presence or absence of ILA in vitro. ILA was added to RAW-Blue cells for 1 h before being exposed to LPS. After incubating for 4 h, SEAP levels were quantified by developing supernatant with QUANTI-Blue substrate for 1 h and reading absorption at 620 nm as stated in the manufacturer's instructions (InvioGen). Caco-2 and HT-29 cells were purchased from ATCC and grown to the specifications. To assess IL-8 production in response to LPS, Caco-2 cells were pre-incubated with ILA for 1 h before

overnight exposure to LPS. For gene expression experiments, cells were incubated with ILA in the presence of TNF- α for 1 h or pretreated with AhR or Nrf2 inhibitors for 1 h before 1 h exposure to ILA. Experiments were performed for a total of 6–8 biological replicates. ILA, AhR antagonist CH-223191, Nrf2 antagonist SML1833, TNF- α and LPS 0111:B4 were purchased from Sigma. GAPDH, anti-rabbit HRP and anti-biotin HRP antibodies were purchased from Cell Signaling Technology. AhR antibody was purchased from Invitrogen. HDAC1 antibody was from Santa Cruz Biotechnologies.

Immunoassays

ELISA Duoset was used to measure IL-8 levels in Caco-2 supernatants according to manufacturer's instructions (R&D Systems).

Western blot

Nuclear and cytosolic fractions were prepared as described previously [69]. Cell lysates were evaluated for total protein content using Bradford assay and overall concentration for each samples adjusted with deionized water and boiled with 2x Laemmli reducing buffer. Individual samples were resolved in SDS-PAGE as per standard protocol. Signals were developed and detected with appropriate antibodies and bands were analyzed using BioRad Imager. GAPDH and HDAC1 were used as internal loading controls for cytosolic and nuclear fractions.

cDNA analysis

Total RNA was extracted from human Caco-2 or HT-29 using TRIzol reagent (Invitrogen) following the manufacturer's instructions. RNA was reverse transcribed with Bio Rad iScript cDNA synthesis kit. cDNA template was combined with PowerUp SYBR Green Master Mix (ThermoFisher) and quantitative PCR was run using Applied Biosystems QuantStudio 6 Real-Time PCR System. Primers used to amplify were cytochrome p450 1a1, glutathione peroxidase 2, superoxide dismutase 2, NAD(P) H dehydrogenase, interleukin-8, beta-defensin2, serotonin transporter, tryptophan-hydroxylase 1, 60S acidic ribosomal protein P13A. Primer sequences are provided in Supplemental Table 2.

Statistical analysis

Student's t test or One-way ANOVA with Bonferroni Multiple comparison test was performed using GraphPad Prism. A *P* value of < 0.05 was considered statistically significant. For ILA dose curves, the mean \pm SEM of relative expression values were fitted with a 3-parameter dose response curve vs the log-transformed ILA concentration (Prism, v. 8.0, GraphPad Software, San Diego, CA). Statistical significance of the effect of each treatment on the means of relative expression of

each target gene at the highest ILA concentration (10 mM) was determined using a one-way ANOVA analysis with a TukeyHSD posthoc comparison (R, version 3.5.2 [70]). For IL-8, the statistical differences between the means in the absence of ILA was also determined by this method. Differences in the homogeneity of microbiota between high and low *Bifidobacterium* groups were determined by using the PERMDISP2 function of R Package Vegan [71] with 999 permutations. Differences in microbial community β -diversity were tested by ADONIS (perMANOVA) in the R Package Vegan. Principal coordinate (PCoA) analysis was carried out by PhyloSeq [72]. Correlation analysis was carried out by Spearman correlation. Statistical analyses were performed by using R version 3.5.2 [70] and Prism, v. 8.0 (GraphPad Software, San Diego, CA). Graphs were prepared by GGplot2 [73] and Prism, v. 8.0 (GraphPad Software, San Diego, CA).

Supplementary Information

The online version contains supplementary material available at <https://doi.org/10.1186/s12866-020-02023-y>.

Additional file 1: Supplemental Figure 1. Metabolites produced by growth of *B. infantis* on lactose or HMO in the differing concentrations of tryptophan. **Supplemental Table 1.** Composition of milk oligosaccharide. **Supplemental Table 2.** Primer sequences. **Supplemental Table 3.** Summary of statistics from TukeyHSD posthoc comparisons of ILA dose responses.

Authors' contributions

HER, DAM, CBS, CS, AME, BMH, and ARP designed the studies. DB provided the HMO and analyzed purity. AME, BMH, ARP, DT, GX, MNH, DM performed the studies and generated the data; AME, BMH, ARP, DT, GX, MNH, DM and MLG analyzed data and prepared for publication. HER, CS, CBL, CBS and DAM contributed to data interpretation. AME, BMH, and ARP wrote the first draft of the manuscript and HER edited and prepared the final draft of the manuscript. All authors read and approved the manuscript.

Funding

This study was funded by National Institutes of Health awards AT006180, AT007079, AT008759 and F32HD093185, and the Peter J. Shields Endowed Chair in Dairy Food Science. This work was funded by WHO Project Number 2010168947 which was funded from the Bill and Melinda Gates Foundation, Thrasher Research Fund grant number 11488 and USDA-ARS Project Number: 2032–53000–001–00-D.

Availability of data and materials

The datasets used and analyzed during the current study are available from the corresponding author on reasonable request.

Ethics approval and consent to participate

The data presented here used of 18 fecal samples originally collected as part of a larger trial of Bangladeshi infants (clinicaltrials.gov identifier: NCT01583972). Procedures for recruitment of subjects have been described previously [58]. Briefly, parents of infants born at the Maternal and Child Health Training Institute in Dhaka, Bangladesh were approached during the third trimester of pregnancy and informed consent was obtained within 48 h of birth. The study was approved by the Ethical Review Committee of the International Centre for Diarrheal Disease Research, Bangladesh (ICDDR,B) and by the Human Studies Committee of the World Health Organization.

Consent for publication

Not applicable.

Competing interests

DAM, DB and CBL are cofounders of Evolve Biosystems, a company focused on diet-based manipulation of the gut microbiota. Evolve Biosystems played no role in the origination, design, execution, interpretation, or publication of this work.

Author details

¹Department of Anatomy, Physiology and Cell Biology, School of Veterinary Medicine, University of California, Davis, CA 95616, USA. ²Foods for Health Institute, University of California, Davis, CA, USA. ³Department of Food Science and Technology, University of CA, Davis, CA, USA. ⁴Department of Chemistry, University of California, Davis, CA, USA. ⁵Enteric and Respiratory Infections Unit, Infectious Diseases Division, icddr,b, Dhaka, Bangladesh. ⁶US Department of Agriculture, Western Human Nutrition Research Center, Davis, CA, USA. ⁷Department of Nutrition, University of California, Davis, CA, USA.

Received: 11 May 2020 Accepted: 27 October 2020

Published online: 23 November 2020

References

- Henrick BM, Yao X-D, Nasser L, Roozrogousheh A, Rosenthal KL. Breastfeeding behaviors and the innate immune system of human Milk: working together to protect infants against inflammation, HIV-1, and other infections. *Front Immunol.* 2017;8:1631. <https://doi.org/10.3389/fimmu.2017.01631>.
- Smilowitz JT, Lebrilla CB, Mills DA, German JB, Freeman SL. Breast milk oligosaccharides: structure-function relationships in the neonate. *Annu Rev Nutr.* 2014;34:143–69. <https://doi.org/10.1146/annurev-nutr-071813-105721>.
- Newburg DS, Ruiz-Palacios GM, Morrow AL. Human milk glycans protect infants against enteric pathogens. *Annu Rev Nutr.* 2005;25:37–58. <https://doi.org/10.1146/annurev-nutr.25.050304.092553>.
- Newburg DS. Glycobiology of human milk. *Biochemistry (Mosc).* 2013;78:771–85. <https://doi.org/10.1134/S0006297913070092>.
- He Y, Lawlor NT, Newburg DS. Human Milk components modulate toll-like receptor-mediated inflammation. *Adv Nutr.* 2016;7:102–11. <https://doi.org/10.3945/an.115.010090>.
- Bode L. Recent advances on structure, metabolism, and function of human milk oligosaccharides. *J Nutr.* 2006;136:2127–30. <https://doi.org/10.1093/jn/136.8.2127>.
- Newburg DS. Oligosaccharides in human milk and bacterial colonization. *J Pediatr Gastroenterol Nutr.* 2000;30(Suppl 2):S8–17. <http://www.ncbi.nlm.nih.gov/pubmed/10749396>.
- German JB, Freeman SL, Lebrilla CB, Mills DA. Human milk oligosaccharides: evolution, structures and bioselectivity as substrates for intestinal bacteria. *Nestle Nutr Workshop Ser Pediatr Program.* 2008;62:205–18; discussion 218–22. <https://doi.org/10.1159/000146322>.
- Yatsunenko T, Rey FE, Manary MJ, Trehan I, Dominguez-Bello MG, Contreras M, et al. Human gut microbiome viewed across age and geography. *Nature.* 2012;486:222–7. <https://doi.org/10.1038/nature11053>.
- Chichlowski M, German JB, Lebrilla CB, Mills DA. The influence of milk oligosaccharides on the microbiota of infants: opportunities for formulas. *Annu Rev Food Sci Technol.* 2011;2:331–51. <https://doi.org/10.1146/annurev-food-022510-133743>.
- LoCascio RG, Ninonuevo MR, Freeman SL, Sela DA, Grimm R, Lebrilla CB, et al. Glycoprofiling of bifidobacterial consumption of human milk oligosaccharides demonstrates strain specific, preferential consumption of small chain glycans secreted in early human lactation. *J Agric Food Chem.* 2007;55:8914–9. <https://doi.org/10.1021/jf0710480>.
- Garrido D, Ruiz-Moyano S, Kirmiz N, Davis JC, Totten SM, Lemay DG, et al. A novel gene cluster allows preferential utilization of fucosylated milk oligosaccharides in *Bifidobacterium longum* subsp. *longum* SC596. *Sci Rep.* 2016;6:35045. <https://doi.org/10.1038/srep35045>.
- Marcobal A, Barboza M, Froehlich JW, Block DE, German JB, Lebrilla CB, et al. Consumption of human milk oligosaccharides by gut-related microbes. *J Agric Food Chem.* 2010;58:5334–40. <https://doi.org/10.1021/jf9044205>.
- Frese SA, Hutton AA, Contreras LN, Shaw CA, Palumbo MC, Casaburi G, et al. Persistence of Supplemental *Bifidobacterium longum* subsp. *infantis* EVC001 in Breastfed Infants. *mSphere.* 2017;2:e00501–17. <https://doi.org/10.1128/mSphere.00501-17>.
- Tanabe S, Kinuta Y, Saito Y. *Bifidobacterium infantis* suppresses proinflammatory interleukin-17 production in murine splenocytes and dextran sodium sulfate-induced intestinal inflammation. *Int J Mol Med.* 2008;22:181–5. <http://www.ncbi.nlm.nih.gov/pubmed/18636171>.
- Sheil B, MacSharry J, O'Callaghan L, O'Riordan A, Waters A, Morgan J, et al. Role of interleukin (IL-10) in probiotic-mediated immune modulation: an assessment in wild-type and IL-10 knock-out mice. *Clin Exp Immunol.* 2006;144:273–80. <https://doi.org/10.1111/j.1365-2249.2006.03051.x>.
- Wickramasinghe S, Pacheco AR, Lemay DG, Mills DA. *Bifidobacteria* grown on human milk oligosaccharides downregulate the expression of inflammation-related genes in Caco-2 cells. *BMC Microbiol.* 2015;15:172. <https://doi.org/10.1186/s12866-015-0508-3>.
- Chichlowski M, De Lartigue G, German JB, Raybould HE, Mills DA. *Bifidobacteria* isolated from infants and cultured on human milk oligosaccharides affect intestinal epithelial function. *J Pediatr Gastroenterol Nutr.* 2012;55:321–7. <https://doi.org/10.1097/MPG.0b013e31824fb899>.
- Aragozzini F, Ferrari A, Pacini N, Gualandris R. Indole-3-lactic acid as a tryptophan metabolite produced by *Bifidobacterium* spp. *Appl Environ Microbiol.* 1979;38:544–6. <https://doi.org/10.1128/AEM.38.3.544-546.1979>.
- Fukuda S, Toh H, Hase K, Oshima K, Nakanishi Y, Yoshimura K, et al. *Bifidobacteria* can protect from enteropathogenic infection through production of acetate. *Nature.* 2011;469:543–7. <https://doi.org/10.1038/nature09646>.
- Derrien M, Veiga P. Rethinking diet to aid human-microbe Symbiosis. *Trends Microbiol.* 2017;25:100–12. <https://doi.org/10.1016/j.tim.2016.09.011>.
- Vernocchi P, Del Chierico F, Putignani L. Gut microbiota profiling: metabolomics based approach to unravel compounds affecting human health. *Front Microbiol.* 2016;7:1144. <https://doi.org/10.3389/fmicb.2016.01144>.
- Huda MN, Ahmad SM, Alam MJ, Khanam A, Kalanetra KM, Taft DH, et al. *Bifidobacterium* abundance in early infancy and vaccine response at 2 years of age. *Pediatrics.* 2019;143:e20181489. <https://doi.org/10.1542/peds.2018-1489>.
- Palframan RJ, Gibson GR, Rastall RA. Carbohydrate preferences of *Bifidobacterium* species isolated from the human gut. *Curr Issues Intest Microbiol.* 2003;4:71–5. <http://www.ncbi.nlm.nih.gov/pubmed/14503691>.
- Liang H, Dai Z, Liu N, Ji Y, Chen J, Zhang Y, et al. Dietary L-tryptophan modulates the structural and functional composition of the intestinal microbiome in weaned piglets. *Front Microbiol.* 2018;9:1736. <https://doi.org/10.3389/fmicb.2018.01736>.
- Zelante T, Iannitti RG, Cunha C, De Luca A, Giovannini G, Pieraccini G, et al. Tryptophan catabolites from microbiota engage aryl hydrocarbon receptor and balance mucosal reactivity via interleukin-22. *Immunity.* 2013;39:372–85. <https://doi.org/10.1016/j.immuni.2013.08.003>.
- Lanis JM, Alexeev EE, Curtis VF, Kitzenberg DA, Kao DJ, Battista KD, et al. Tryptophan metabolite activation of the aryl hydrocarbon receptor regulates IL-10 receptor expression on intestinal epithelia. *Mucosal Immunol.* 2017;10:1133–44. <https://doi.org/10.1038/mi.2016.133>.
- Agus A, Planchais J, Sokol H. Gut microbiota regulation of tryptophan metabolism in health and disease. *Cell Host Microbe.* 2018;23:716–24. <https://doi.org/10.1016/j.chom.2018.05.003>.
- Lamas B, Natividad JM, Sokol H. Aryl hydrocarbon receptor and intestinal immunity. *Mucosal Immunol.* 2018;11:1024–38. <https://doi.org/10.1038/s41385-018-0019-2>.
- Henrick BM, Yao X-D, Rosenthal KL, INFANT study team. HIV-1 Structural Proteins Serve as PAMPs for TLR2 Heterodimers Significantly Increasing Infection and Innate Immune Activation. *Front Immunol.* 2015;6:426. <https://doi.org/10.3389/fimmu.2015.00426>.
- van der Bruggen T, Nijenhuis S, van Raaij E, Verhoeve J, van Asbeck BS. Lipopolysaccharide-induced tumor necrosis factor alpha production by human monocytes involves the raf-1/MEK1-MEK2/ERK1-ERK2 pathway. *Infect Immun.* 1999;67:3824–9. <http://www.ncbi.nlm.nih.gov/pubmed/10417144>.
- Rothhammer V, Mascanfroni ID, Bunsle L, Takenaka MC, Kenison JE, Mayo L, et al. Type I interferons and microbial metabolites of tryptophan modulate astrocyte activity and central nervous system inflammation via the aryl hydrocarbon receptor. *Nat Med.* 2016;22:586–97. <https://doi.org/10.1038/nm.4106>.
- Ikuta T, Kobayashi Y, Kawajiri K. Cell density regulates intracellular localization of aryl hydrocarbon receptor. *J Biol Chem.* 2004;279:19209–16. <https://doi.org/10.1074/jbc.M310492200>.
- Hayes JD, Dinkova-Kostova AT, McMahon M. Cross-talk between transcription factors AhR and Nrf2: lessons for cancer chemoprevention from dioxin. *Toxicol Sci.* 2009;111:199–201. <https://doi.org/10.1093/toxsci/kfp168>.
- Henrick BM, Chew S, Casaburi G, Brown HK, Frese SA, Zhou Y, et al. Colonization by *B. infantis* EVC001 modulates enteric inflammation in exclusively breastfed infants. *Pediatr Res.* 2019;86:749–57. <https://doi.org/10.1038/s41390-019-0533-2>.

36. Underwood MA, Arriola J, Gerber CW, Kaveti A, Kalanetra KM, Kananurak A, et al. *Bifidobacterium longum* subsp. *infantis* in experimental necrotizing enterocolitis: alterations in inflammation, innate immune response, and the microbiota. *Pediatr Res*. 2014;76:326–33. <https://doi.org/10.1038/pr.2014.102>.
37. Zivkovic AM, Barile D. Bovine milk as a source of functional oligosaccharides for improving human health. *Adv Nutr*. 2011;2:284–9. <https://doi.org/10.3945/an.111.000455>.
38. Riedel C-U, Foata F, Philippe D, Adolfsson O, Eikmanns B-J, Blum S. Anti-inflammatory effects of bifidobacteria by inhibition of LPS-induced NF-kappaB activation. *World J Gastroenterol*. 2006;12:3729–35. <https://doi.org/10.3748/wjg.v12.i23.3729>.
39. McCarthy J, O'Mahony L, O'Callaghan L, Sheil B, Vaughan EE, Fitzsimons N, et al. Double blind, placebo controlled trial of two probiotic strains in interleukin 10 knockout mice and mechanistic link with cytokine balance. *Gut*. 2003;52:975–80. <https://doi.org/10.1136/gut.52.7.975>.
40. Okey AB, Riddick DS, Harper PA. The ah receptor: mediator of the toxicity of 2,3,7,8-tetrachlorodibenzo-p-dioxin (TCDD) and related compounds. *Toxicol Lett*. 1994;70:1–22. [https://doi.org/10.1016/0378-4274\(94\)90139-2](https://doi.org/10.1016/0378-4274(94)90139-2).
41. Metidji A, Omenetti S, Crotta S, Li Y, Nye E, Ross E, et al. The Environmental Sensor AHR Protects from Inflammatory Damage by Maintaining Intestinal Stem Cell Homeostasis and Barrier Integrity. *Immunity*. 2018;49:353–62.e5. <https://doi.org/10.1016/j.immuni.2018.07.010>.
42. Schiering C, Wincent E, Metidji A, Iseppon A, Li Y, Potocnik AJ, et al. Feedback control of AHR signalling regulates intestinal immunity. *Nature*. 2017;542:242–5. <https://doi.org/10.1038/nature21080>.
43. Gill PA, van Zelm MC, Muir JG, Gibson PR. Review article: short chain fatty acids as potential therapeutic agents in human gastrointestinal and inflammatory disorders. *Aliment Pharmacol Ther*. 2018;48:15–34. <https://doi.org/10.1111/apt.14689>.
44. Gandhi R, Kumar D, Burns EJ, Nadeau M, Dake B, Laroni A, et al. Activation of the aryl hydrocarbon receptor induces human type 1 regulatory T cell-like and Foxp3(+) regulatory T cells. *Nat Immunol*. 2010;11:846–53. <https://doi.org/10.1038/ni.1915>.
45. Potapovich AI, Lulli D, Fidanza P, Kostyuk VA, De Luca C, Pastore S, et al. Plant polyphenols differentially modulate inflammatory responses of human keratinocytes by interfering with activation of transcription factors NFkB and AhR and EGFR-ERK pathway. *Toxicol Appl Pharmacol*. 2011;255:138–49. <https://doi.org/10.1016/j.taap.2011.06.007>.
46. Meng D, Sommella E, Salviati E, Campiglia P, Ganguli K, Djebali K, et al. Indole-3-lactic acid, a metabolite of tryptophan, secreted by *Bifidobacterium longum* subspecies *infantis* is anti-inflammatory in the immature intestine. *Pediatr Res*. 2020;88:209–17. <https://doi.org/10.1038/s41390-019-0740-x>.
47. Konieczna P, Groeger D, Ziegler M, Frei R, Ferstl R, Shanahan F, et al. *Bifidobacterium infantis* 35624 administration induces Foxp3 T regulatory cells in human peripheral blood: potential role for myeloid and plasmacytoid dendritic cells. *Gut*. 2012;61:354–66. <https://doi.org/10.1136/gutjnl-2011-300936>.
48. Ma Q. Role of nrf2 in oxidative stress and toxicity. *Annu Rev Pharmacol Toxicol*. 2013;53:401–26. <https://doi.org/10.1146/annurev-pharmtox-011112-140320>.
49. Innamorato NG, Rojo AI, García-Yagüe AJ, Yamamoto M, de Ceballos ML, Cuadrado A. The transcription factor Nrf2 is a therapeutic target against brain inflammation. *J Immunol*. 2008;181:680–9. <https://doi.org/10.4049/jimmunol.181.1.680>.
50. Song M-Y, Kim E-K, Moon W-S, Park J-W, Kim H-J, So H-S, et al. Sulforaphane protects against cytokine- and streptozotocin-induced beta-cell damage by suppressing the NF-kappaB pathway. *Toxicol Appl Pharmacol*. 2009;235:57–67. <https://doi.org/10.1016/j.taap.2008.11.007>.
51. Kamimura S, Eguchi K, Sekiba K. Tryptophan and its metabolite concentrations in human plasma and breast milk during the perinatal period. *Acta Med Okayama*. 1991;45:101–6. <https://doi.org/10.18926/AMO/32183>.
52. Bischoff SC, Mailer R, Pabst O, Weier G, Sedlik W, Li Z, et al. Role of serotonin in intestinal inflammation: knockout of serotonin reuptake transporter exacerbates 2,4,6-trinitrobenzene sulfonic acid colitis in mice. *Am J Physiol Gastrointest Liver Physiol*. 2009;296:G685–95. <https://doi.org/10.1152/ajpgi.90685.2008>.
53. Coates MD, Mahoney CR, Linden DR, Sampson JE, Chen J, Blaszyk H, et al. Molecular defects in mucosal serotonin content and decreased serotonin reuptake transporter in ulcerative colitis and irritable bowel syndrome. *Gastroenterology*. 2004;126:1657–64. <https://doi.org/10.1053/j.gastro.2004.03.013>.
54. Wehkamp J, Fellermann K, Herrlinger KR, Baxmann S, Schmidt K, Schwind B, et al. Human beta-defensin 2 but not beta-defensin 1 is expressed preferentially in colonic mucosa of inflammatory bowel disease. *Eur J Gastroenterol Hepatol*. 2002;14:745–52. <https://doi.org/10.1097/00042737-200207000-00006>.
55. Gersemann M, Wehkamp J, Fellermann K, Stange EF. Crohn's disease—defect in innate defence. *World J Gastroenterol*. 2008;14:5499–503. <https://doi.org/10.3748/wjg.14.5499>.
56. Wang C, Jiang Y, Ma J, Wu H, Wacker D, Katritch V, et al. Structural basis for molecular recognition at serotonin receptors. *Science*. 2013;340:610–4. <https://doi.org/10.1126/science.1232807>.
57. Schwab M, Reynnders V, Loitsch S, Steinhilber D, Schröder O, Stein J. The dietary histone deacetylase inhibitor sulforaphane induces human beta-defensin-2 in intestinal epithelial cells. *Immunology*. 2008;125:241–51. <https://doi.org/10.1111/j.1365-2567.2008.02834.x>.
58. Huda MN, Lewis Z, Kalanetra KM, Rashid M, Ahmad SM, Raqib R, et al. Stool microbiota and vaccine responses of infants. *Pediatrics*. 2014;134:e362–72. <https://doi.org/10.1542/peds.2013-3937>.
59. Huda MN, Ahmad SM, Kalanetra KM, Taft DH, Alam MJ, Khanam A, et al. Neonatal vitamin a supplementation and vitamin a status are associated with gut microbiome composition in Bangladeshi infants in early infancy and at 2 years of age. *J Nutr*. 2019;149:1075–88. <https://doi.org/10.1093/jn/nxz034>.
60. Ahmad SM, Raqib R, Huda MN, Alam MJ, Monirujjaman M, Akhter T, et al. High-dose neonatal vitamin a supplementation transiently decreases Thymic function in early infancy. *J Nutr*. 2020;150:176–83. <https://doi.org/10.1093/jn/nxz193>.
61. Caporaso JG, Lauber CL, Walters WA, Berg-Lyons D, Huntley J, Fierer N, et al. Ultra-high-throughput microbial community analysis on the Illumina HiSeq and MiSeq platforms. *ISME J*. 2012;6:1621–4. <https://doi.org/10.1038/ismej.2012.8>.
62. Caporaso JG, Kuczynski J, Stombaugh J, Bittinger K, Bushman FD, Costello EK, et al. QIIME allows analysis of high-throughput community sequencing data. *Nat Methods*. 2010;7:335–6. <https://doi.org/10.1038/nmeth.f.303>.
63. McDonald D, Price MN, Goodrich JK, Nawrocki EP, DeSantis TZ, Probst A, et al. An improved Greengenes taxonomy with explicit ranks for ecological and evolutionary analyses of bacteria and archaea. *ISME J*. 2012;6:610–8. <https://doi.org/10.1038/ismej.2011.139>.
64. Rivera-Chávez F, Zhang LF, Faber F, Lopez CA, Byndloss MX, Olsan EE, et al. Depletion of Butyrate-Producing Clostridia from the Gut Microbiota Drives an Aerobic Luminal Expansion of Salmonella Cell Host Microbe 2016; 19(4): 443–454.
65. de Moura BJMLN, Cohen JL, de Aquino LFMC, Lee H, de Melo Silva VL, Liu Y, et al. An integrated bioprocess to recover bovine Milk oligosaccharides from colostrum whey permeate. *J Food Eng*. 2018;216:27–35. <https://doi.org/10.1016/j.jfoodeng.2017.07.022>.
66. Lee H, de MeloSilva VL, Liu Y, Barile D. Short communication: quantification of carbohydrates in whey permeate products using high-performance anion-exchange chromatography with pulsed amperometric detection. *J Dairy Sci*. 2015;98:7644–9. <https://doi.org/10.3168/jds.2015-9882>.
67. Smart KF, Aggio RBM, Van Houtte JR, Villas-Bôas SG. Analytical platform for metabolome analysis of microbial cells using methyl chloroformate derivatization followed by gas chromatography-mass spectrometry. *Nat Protoc*. 2010;5:1709–29. <https://doi.org/10.1038/nprot.2010.108>.
68. He X, Mishchuk DO, Shah J, Weimer BC, Slupsky CM. Cross-talk between E coli strains and a human colorectal adenocarcinoma-derived cell line. *Sci Rep*. 2013;3:3416. <https://doi.org/10.1038/srep03416>.
69. Beg AA, Finco TS, Nantermet PV, Baldwin AS. Tumor necrosis factor and interleukin-1 lead to phosphorylation and loss of I kappa B alpha: a mechanism for NF-kappa B activation. *Mol Cell Biol*. 1993;13:3301–10. <https://doi.org/10.1128/mcb.13.6.3301>.
70. R Core Team. R: A Language and Environment for Statistical Computing. Vienna, Austria; 2020. <https://www.r-project.org/>.
71. Oksanen J, Blanchet FG, Friendly M, Kindt R, Legendre P, McGlenn D, et al. *vegan: Community Ecology Package*. 2019. <https://cran.r-project.org/package=vegan>.
72. McMurdie PJ, Holmes S. phyloseq: an R package for reproducible interactive analysis and graphics of microbiome census data. *PLoS One*. 2013;8:e61217. <https://doi.org/10.1371/journal.pone.0061217>.
73. Wickham H. *ggplot2: Elegant Graphics for Data Analysis*. Springer-Verlag New York; 2016. <https://ggplot2.tidyverse.org>.

Publisher's Note

Springer Nature remains neutral with regard to jurisdictional claims in published maps and institutional affiliations.